


## Article

# Variability in Microbial Communities Driven by Particulate Matter on Human Facial Skin

Kai Fu <sup>1,2</sup>, Qixing Zhou <sup>2,\*</sup>  and Heli Wang <sup>1</sup>

<sup>1</sup> School of Water Resources and Environment, China University of Geosciences (Beijing), Beijing 100083, China; fukai1998@126.com (K.F.)

<sup>2</sup> Key Laboratory of Pollution Processes and Environmental Criteria (Ministry of Education), Tianjin Key Laboratory of Environmental Remediation and Pollution Control, Carbon Neutrality Interdisciplinary Science Centre/College of Environmental Science and Engineering, Nankai University, Tianjin 300350, China

\* Correspondence: zhouqx@nankai.edu.cn

**Abstract:** Microbial communities are known to play an important role in maintaining ecological balance and can be used as an indicator for assessing environmental pollution. Numerous studies have revealed that air pollution can alter the structure of microbial communities, which may increase health risks. Nevertheless, the relationships between microbial communities and particulate matter (PM) caused by air pollution in terms of health risk assessment are not well understood. This study aimed to validate the influences of PM chemical compositions on microbial communities and assess the associated health risks. Our results, based on similarity analysis, revealed that the stability structure of the microbial communities had a similarity greater than 73%. In addition, the altered richness and diversity of microbial communities were significantly associated with PM chemical compositions. Volatile organic compounds (VOCs) and polycyclic aromatic hydrocarbons (PAHs) exerted a positive influence on microbial communities in different environmental variables. Additionally, a stronger linear correlation was observed between hydroxyl radicals ( $\cdot\text{OH}$ ) and the richness of microbial communities. All estimated health risks from PM chemical compositions, calculated under different environmental variables, significantly exceeded the acceptable level by a factor of more than 49. Cr and 1,2-Dibromoethane displayed dual adverse effects of non-carcinogenic and carcinogenic risks. Overall, the study provides insights into the fundamental mechanisms of the variability in microbial communities driven by PM, which may support the crucial role of PM chemical compositions in the risk of microorganisms in the atmospheric environment.

**Keywords:** variability; microbial communities; PM; chemical compositions; health risk



**Citation:** Fu, K.; Zhou, Q.; Wang, H. Variability in Microbial Communities Driven by Particulate Matter on Human Facial Skin. *Toxics* **2024**, *12*, 497. <https://doi.org/10.3390/toxics12070497>

Academic Editors: Lía Celina Méndez-Rodríguez and Mahesh Rachamalla

Received: 16 May 2024

Revised: 1 July 2024

Accepted: 2 July 2024

Published: 8 July 2024



**Copyright:** © 2024 by the authors. Licensee MDPI, Basel, Switzerland. This article is an open access article distributed under the terms and conditions of the Creative Commons Attribution (CC BY) license (<https://creativecommons.org/licenses/by/4.0/>).

## 1. Introduction

Air quality in developing countries, particularly in the Beijing–Tianjin–Hebei Region in China, has become a major concern in recent years, with the connection between air pollution and human health recently obtaining increasing attention based on the findings of several environmental toxicology experiments [1,2]. Human lifestyle, customs, and income levels have led to long-term exposure to outdoor air pollution with higher concentrations of particulate matter (PM), despite conscious efforts to adopt protective measures [3,4]. Previous studies have reported a higher health risk associated with exposure to high concentrations of PM, which increases with unsatisfactory protective measures and weaker individual physiques [5,6]. In addition, given that the face, encompassing the ears, eyes, nose, and mouth, serves as the primary entry point for PM and airborne bacteria into the human body [7,8], it is essential to understand the concentrations of PM, PM chemical compositions, and microbial communities on human facial skin to assess human health risks, regulate air pollution, and improve individual protective measures.

Although every human has their own characterized microbial cloud (microbial communities), a ubiquitous part of the environment, the microbial communities may change as

environmental variables such as temperature, humidity, illumination, salinity, pH, etc., are altered [9–11]. Changes in microbial communities, including alterations in their concentrations and richness, have been linked to inflammatory diseases, immune responses, and chronic respiratory illnesses, such as asthma and allergic dermatitis [12,13].

Several studies have revealed correlations between microbial communities and PM chemical compositions and reported that these compositions played a significant role in the variability, richness, and diversity of microbial communities [14–16]. Laboratory research further demonstrated that heavy metals and polycyclic aromatic hydrocarbons (PAHs) can inhibit or promote the growth of microbial communities, depending on their concentrations and types [17,18]. These studies also suggested that heavy metals, water-soluble anions, PAHs, and volatile organic compounds (VOCs) may enhance the attenuation of bacteria if these toxic pollutants are utilized as carbon or nitrogen sources, or if they induce changes in DNA, enzymes, or albumin [12,19,20]. Mechanistic investigations have revealed the critical role of hydroxyl radicals ( $\cdot\text{OH}$ ) in regulating microbial communities, which may influence their richness and diversity [21]. Moreover, it has been suggested that  $\cdot\text{OH}$  radicals may induce substantial changes in microbial communities through metabolic processes, ultimately leading to cellular inactivation [22]. Although numerous studies have been conducted on microbial communities and PM from different separate or mutual perspectives, few studies have assessed the relationship between microbial communities and PM on human facial skin [14,23].

Considering the significant influence of factors such as PM concentrations and temporal variation on the variability in microbial communities driven by PM on human facial skin, it is crucial to examine microbial communities under different PM concentrations and at different times on the human facial skin [24,25]. This would enable the evaluation of environmental risks, determination of associations between PM chemical compositions and microbial communities and development of effective individual protective measures for use in daily life and scientific research.

High-throughput barcoded pyrosequencing of the 16S rRNA gene has been used to detect microbial communities; presently, PM chemical compositions are highly variable in different locations with diverse emission sources through analysis and detection methods that are well-established in the existing literatures [26–29]. In the present study, canonical correspondence analysis (CCA) combined with orthogonal partial least squares discriminant analysis (OPLS-DA) was used to investigate the association between microbial communities and PM chemical compositions on human facial skin. In addition, linear fitting based on the area of facial skin was used to determine the effects of  $\cdot\text{OH}$  by electron paramagnetic resonance (EPR) on the microbial communities.

In this study, we combined PM chemical compositions and microbial communities to describe the compositions and variability in bacterial communities, then determined their correlation on human facial skin at different concentrations of PM and times. Lastly, the health risks associated with exposure to PM were calculated to provide insights for developing novel preventive methods for treating pollutants and formulating measures to minimize the adverse effects caused by PM.

## 2. Materials and Methods

### 2.1. Samples Collection

The samples were collected from college students as fixed sample takers who shared similar characteristics in terms of age (20 to 22 years old), daily routine, diet, and access to air conditioning in Tianjin, China (39°10' N, 117°10' E). A total of 480 samples were collected in winter at two distinct times during the day: in the morning after waking up (08:00) and in the evening before sleeping (22:00). These samples were categorized based on two types of air quality conditions: high ( $>75 \mu\text{g}/\text{m}^3$ , corresponding to an air pollution index of level three or above in China) and low ( $\leq 75 \mu\text{g}/\text{m}^3$ , corresponding to an air pollution index below level three in China) concentrations of  $\text{PM}_{2.5}$ . To exclude the influence of epidermis and secretions (sweat, fat, etc.) on the results, the students were advised to thoroughly

clean their facial skin one hour before morning sampling. Furthermore, samples were collected in the morning and evening periods, ensuring a stable and long exposure time (approximately 15 h per day) and increasing resistance to fluctuating environmental factors such as ozone, UV light, temperature, and humidity. Sterilized medical cotton balls made of absorbent cotton balls (Aladdin, Shanghai, China) were uniformly applied to the surface of the facial skin for collecting PM chemical compositions and microbial communities. In instances free of contamination, a medical cotton ball served as a negative control.

The body surface area was calculated using height and weight parameters based on the Stevenson formula [30,31]. Then, the area of facial skin was calculated using the “Rule of Nines” [32,33]. The specific computational formula is described as follows:

$$S = \frac{0.0061 \times \text{Height} + 0.0128 \times \text{Weight} - 0.1529}{9} \quad (1)$$

where S represents the area of facial skin (m<sup>2</sup>), height represents the body height (cm), and weight represents the body weight (kg).

A summary of air quality information for the samples was obtained from the China National Environmental Monitoring Centre (CNEMC) and release PM monitoring data on a 1 h cycle. The summary of the sampling collection information is described in Table 1.

**Table 1.** Summary of the sampling collection information.

Samples Collection	Concentrations of PM <sub>2.5</sub> /μg/m <sup>3</sup>	Concentrations of PM <sub>10</sub> /μg/m <sup>3</sup>
High concentrations of PM	139	183
	207	290
	166	202
	160	196
	39	54
Low concentrations of PM	45	79
	27	50
	49	85

### 2.2. 16S rRNA Gene Amplification and Sequencing Processing

Half of each sample was cut into small pieces, and the whole genomic DNA was extracted using an E.Z.N.A.<sup>®</sup> Soil DNA Kit (Omega Bio-tek, Norcross, GA, USA), following the manufacturer’s protocols. The DNA was extracted in triplicate, and the extracts from the same sample were pooled together and detected using 1% agarose gel electrophoresis. Polymerase chain reaction (PCR, ABI GeneAmp<sup>®</sup> 9700, Foster City, CA, USA) with the primer sets 515F (5'-barcode-GTGCCAGCMGCCCGG-3') and 907R (5'-CCGTCAATTCMTTTRAGTTT-3') was used to amplify the 16S rRNA gene in the V4–V5 hypervariable regions. Quantitative PCR was performed using the QuantiFluor<sup>™</sup>-ST (Promega, Fitchburg, WI, USA) blue fluorescence quantitative system after the 16S rRNA gene was amplified. Each process run included a non-template control to assess contamination. The purified amplified samples were sequenced using the Illumina MiSeq platform [34,35]. Operational taxonomic units (OTUs) with a 97% similarity threshold were identified based on classification at seven taxonomic ranks of the Ribosomal Database Project (RDP) classifier. These operations were conducted at Majorbio Biopharm Technology Co., Ltd. (Shanghai, China), and the detailed methods are provided in the Supplementary Materials.

### 2.3. Analysis of Particulate Matter Chemical Compositions

Half of each sample was prepared for PM chemical composition analysis. Briefly, the samples were immersed in 20 mL of ultrapure water for 120 min and then subjected to extraction for 60 min using an ultrasonic bath (KQ-500DE, KunShan Ultrasonic Instruments Co., Ltd., Kunshan, China) with 50 W and a shaker at 150 rpm (HYG-A, TaicangHaocheng-ShiyanYiqiZhizao, Co., Ltd., Taicang, China) for 120 min. The original extracted solutions

were obtained after separation by centrifugation (Universal-32R, Heltich, Kirchleugern, Germany) at  $1845 \times g$  for 30 min. The extracted solutions were pooled after two rounds of extraction and filtered through a microporous membrane filter.

Next, a microwave digestion system (MDS-8 Sineo Microwave Chemistry Technology Co., Ltd., Shanghai, China) was used to digest the samples. Additionally, 14 typical heavy metals (Al, As, Ca, Cd, Co, Cr, Cu, Fe, Hg, Mn, Ni, Pb, Sr, and Zn), 4 anions ( $\text{SO}_4^{2-}$ ,  $\text{NO}_3^-$ ,  $\text{Cl}^-$ , and  $\text{F}^-$ ) of water-soluble ions, 16 priority PAHs, and 35 VOCs were analyzed and quantified. The assessment of heavy metals, water-soluble ions, PAHs, and VOCs was performed as previously reported [14], and the detailed descriptions are presented in the Supplementary Materials (Tables S1 and S2).

#### 2.4. Electron Paramagnetic Resonance

The generation of  $\cdot\text{OH}$  through a Fenton-type reaction, as a means to assess oxidative stress caused by PM, was performed as previously described [36–38]. Briefly, 0.5 mL of the extracted solution was placed in a vial with 25  $\mu\text{L}$  of 500 mM 5,5-dimethyl-1-pyrroline-N-oxide (DMPO, Aladdin, Shanghai, China) as a spin trap; 50  $\mu\text{L}$  of 250 mM  $\text{H}_2\text{O}_2$  was then incubated for 30 min at room temperature in an ultrasonic bath with 50 W after adequately shaking with shaker and vortex mixer. The incubated suspension was transferred into an EPR capillary tube, sealed, and then analyzed using MiniScope-400 EPR spectrometer (Magnettech, Berlin, Germany).

#### 2.5. Health Risk Assessment

Health risks from polluted air were considered the chemical compositions of PM with dermal contact route on human facial skin. The dose dermal absorption was estimated by Equation (2) according to the Human Health Evaluation Manual from US EPA [8,39]:

$$D_{\text{dermal}} = \frac{C \times AF \times SA \times ABS \times ED \times EF}{BW \times AT} \quad (2)$$

where C represents the concentrations of PM chemical compositions ( $\mu\text{g}/\text{m}^3$ ); AF represents the dermal adherence factors ( $\text{mg}/\text{cm}^2$ ); SA represents the total exposed skin surface area ( $\text{cm}^2$ ); ABS represents the dermal absorption factor; ED represents the exposure duration (years); EF represents the exposure frequency (days/years); BW represents body weight (kg); and AT represents the averaging lifetime (days). The values and units of these parameters are listed in Table 2. The concentrations of PM chemical compositions were determined by an average air flow rate of 8 L/s with ventilation indoors and an average exposure duration of 18 h/day [40].

Non-carcinogenic risk is typically assessed using hazard quotient (HQ). For substances classified as non-carcinogenic, an HQ exceeding 1 indicates a potential for adverse effects. HQ is calculated using Equation (3):

$$HQ = \frac{D_{\text{dermal}}}{\text{RfD}} \quad (3)$$

where RfD is chronic reference dose for PM chemical compositions ( $\text{mg}/\text{kg}/\text{day}$ ) [8,41].

CR is expressed by the product of the dermal absorption dose and the carcinogenic slope factor (SF):

$$CR = D_{\text{dermal}} \times SF \quad (4)$$

where SF is the carcinogenicity slope factor ( $\text{mg}/\text{kg}/\text{day}$ ) [41,42].

**Table 2.** Exposure parameter values used in the dose dermal absorption calculations [43,44].

Model Parameters	Abbreviations	Values
Dermal adherence factors	AF	2000 mg/m <sup>2</sup>
Dermal absorption factor	ABS	0.13
Total exposed skin area	SA	m <sup>2</sup>
Exposure duration	ED	25 years
Exposure frequency	EF	313 days/year
Body weight	BW	kg
Averaging time	AT	25,550 days

### 2.6. Statistical Analysis

Singleton sequences were discarded after the process of finding unique sequences was implemented to decrease the redundant computation burden of the analysis procedure. Based on cluster information, the richness estimator and the diversity index were obtained using MOTHUR (<http://www.mothur.org/>, accessed on 4 March 2023), with a 97% identity threshold. Sorensen community similarity coefficients were calculated to define the community similarity in different environmental variables. All analyses were conducted in three independent experiments with error bars representing standard deviation (mean  $\pm$  SD). CCA performed in Canoco 5 was used to relate the microbial communities to PM chemical compositions. Collinear variables were removed before the analyses according to Collinearity Diagnostics using the SPSS software (V29), and CCA models were simplified by removing non-significant PM chemical composition variables. A weighted correlation matrix from CCA models was used to relate the effects of PM chemical composition variations that quantify the variation explained and controlled for the effects separately. Further, variable importance in the projection (VIP) and coefficient CS analysis of OPLS-DA were conducted using SIMCA-P+ 14.0 to filter the effects of chemical compositions combined with CCA models. The effects of ·OH on the microbial communities were evaluated using linear fitting based on the facial skin area. A paired-samples t-test was performed to measure the *p* values, and the criteria for significance were set at *p* < 0.05.

## 3. Results

### 3.1. The Variability in Microbial Community Structure

After discarding non-significant sequences, the total number of optimized sequences as reads obtained in each sample ranged from 21,729 to 37,278. Using a 97% similarity threshold, we identified 94–133 OTUs. The paired-sample t-test demonstrated a non-significant difference in OTUs between the samples from high and low PM concentrations (*p* > 0.55). Furthermore, the same result was obtained from the morning and evening samples (*p* > 0.66), indicating no significant difference in the number of OTUs between these time points. However, the number of OTUs increased with increasing concentrations of PM. Interestingly, a similar phenomenon was observed in the morning samples, with higher OTUs observed than in the evening samples. There were  $\geq 45$  shared OTUs in all samples. In both morning and evening samples, high PM concentrations were found to be the most abundant shared OTUs, indicating that the microbial communities might have a close association with high PM concentrations (Figure 1). The richness and diversity of microbial communities were investigated to explore the differences in microbial communities among the different samples without taking into account the time required. The findings showed that the Chao indexes were larger in samples collected during high concentrations of PM than those collected during low concentrations of PM (*p* = 0.02), indicating that the richness of microorganisms was higher in high concentrations of PM (Figure 2). Additionally, there were significant differences (*p* = 0.03) in the Shannon index between the two concentrations of PM, with higher diversity observed in higher concentrations of PM. Similar results were found between the morning and evening samples, with Chao and Shannon indexes indicating that microbial communities had higher richness and lower diversity in the morning samples (Figure 2). Both the Chao (*p* = 0.05) and Shannon (*p* = 0.04) indexes were

significantly different between the morning and evening samples. The observed species were more abundant in higher concentrations of PM and in the morning, although the differences were not significant ( $p > 0.60$ ) (Figure 2). Collectively, these findings suggest that both concentrations of PM and temporal variations had an important influence on microbial communities on human facial skin.

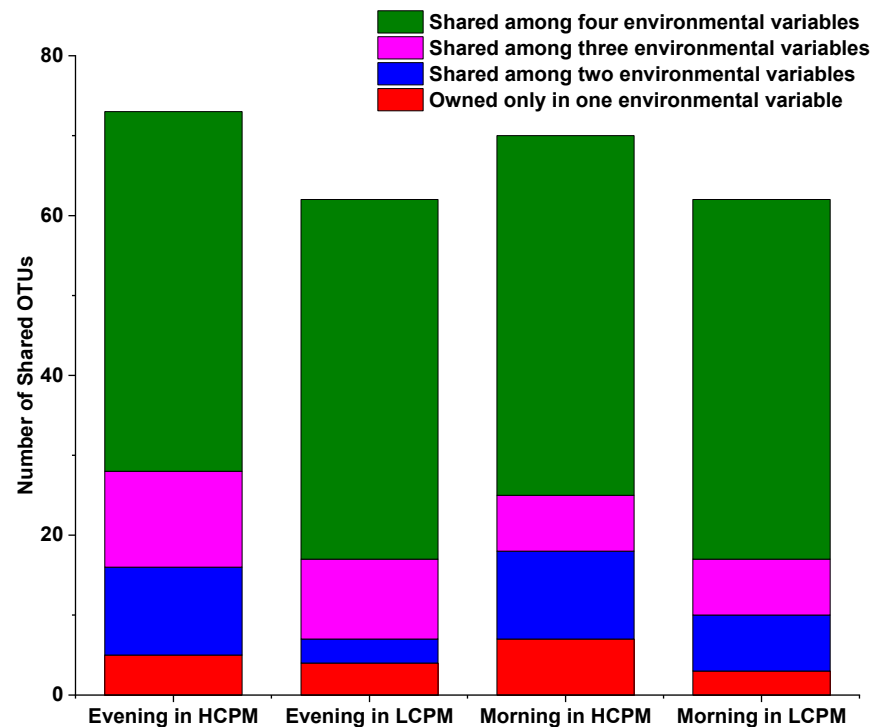


**Figure 1.** Shared OTUs between different environmental variables during the morning and evening: high concentrations of PM (HCPM) and low concentrations of PM (LCPM).

The taxonomic classification of bacteria based on the taxonomic rank of the RDP classifier was implemented for characterizing microbial community structure. The microbial community structure showed a low variability in all samples (Figure 3). *Lactobacillales*, *Bacillales*, *Solibacillus*, and *Pseudomonadales* were the most abundant bacterial taxa, comprising approximately 83% of all communities. To further explore the variability in the microbial community in different concentrations of PM and at different times, the modified Sorensen community similarity coefficients were calculated using the following calculation formula assisting similarity [45,46]:

$$S = \frac{2c}{a + b} \quad (5)$$

where S represents the community similarity coefficient; a represents the species in the sample (community) A; b represents the species in the sample (community) B; and c represents the shared species in samples (communities) A and B.

The similarity coefficient in samples collected during high concentrations of PM was 79.61%, which is higher than that in samples collected during low concentrations of PM (73.61%). Similarly, the similarity coefficients in morning and evening samples were 76.66% and 78.20%, respectively, and the Sorensen community similarity coefficients calculated above were in accordance with shared OTUs, as shown in Figure 1. Further, we also observed that the microbial community structure tended to differ more between different concentrations of PM, although the difference was non-significant.

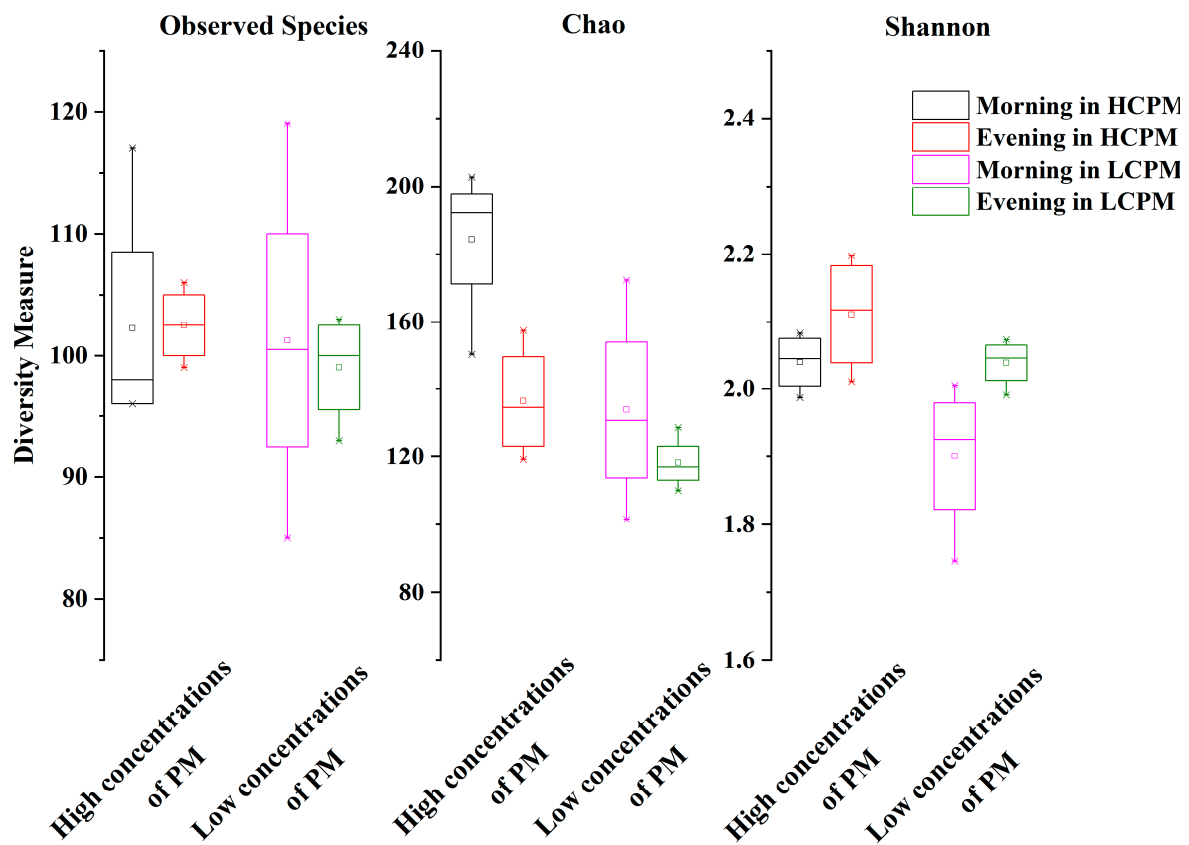


**Figure 2.** Summary of observed species, richness, and diversity associated with different environmental variables displayed in box plots. Observed species and Chao indexes were plotted to measure richness. Shannon index was used to measure diversity. HCPM: high concentrations of PM; LCPM: low concentrations of PM.

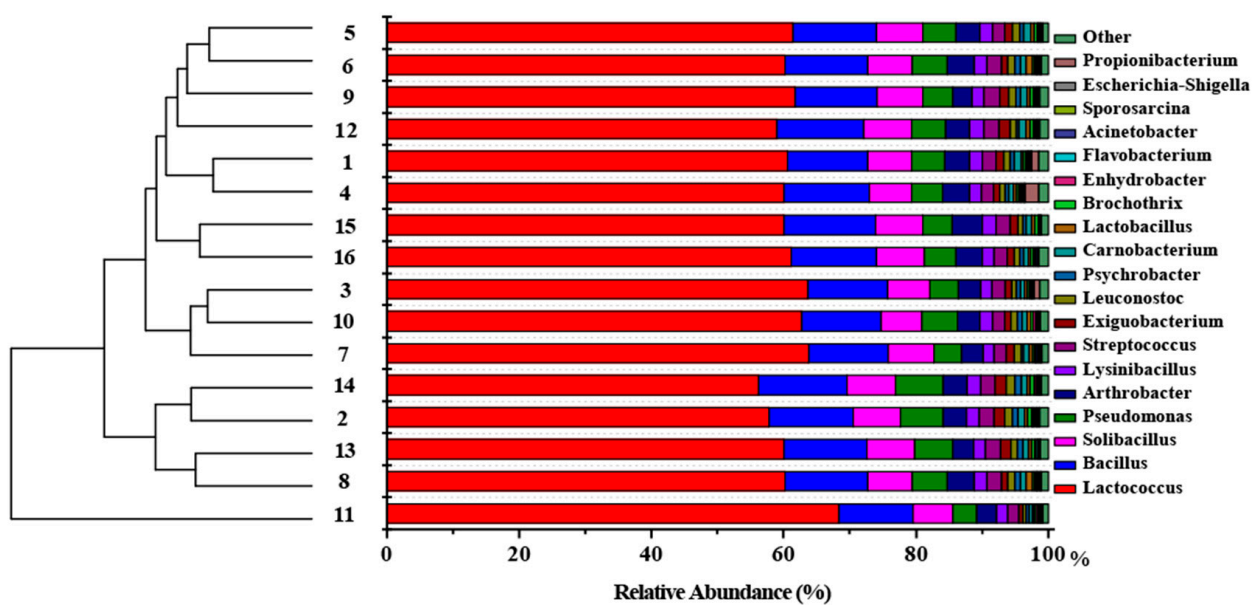


**Figure 3.** Taxonomic composition and similarity of all samples at the genus level. The relative abundance of the genera is listed on the right, and the remaining genera in each library are represented by “others”. The similarity of relative abundance among all samples is displayed on the left.

### 3.2. Relationships between Microbial Communities and Chemical Compositions

The relationships between microbial communities and chemical compositions were analyzed by quantifying 14 typical heavy metals, 4 water-soluble anions, 16 priority PAHs, and 35 VOCs. The results showed that the concentrations of all analyzed chemical compositions analyzed ranged from 74.40 to 254.38 mg/m<sup>2</sup> in the samples collected under different sampling conditions (Table S3). Both richness and diversity indexes were found to decrease with decreasing concentrations of PM, and the morning samples had higher richness and lower diversity (Table S3 and Figure 2), indicating that the structure of microbial communities varied according to the concentrations of PM chemical compositions collected from human facial skin. Eleven effective variables in PM, specifically Ca and Cr of heavy metals, Acenaphthene (Acen), Benzo[k]fluoranthene (BkF), and Indeno[1,2,3-cd]pyrene (InP) of PAHs, Toluene, 1,2-Dibromoethane, Chlorobenzene, p-Xylene, and 1,3,5-Trimethylbenzene of VOCs, and NO<sub>3</sub><sup>-</sup> of water-soluble ions were optimized from all the chemical compositions. After eliminating the collinear variables that showed a strong correlation with other chemical compositions using Collinearity Diagnostics (Tolerance ≤ 0.1 or VIF ≥ 10), the concentrations of the remaining variables, considered effective variables, were analyzed. These concentrations ranged from 0.71 to 2.88 mg/m<sup>2</sup>, constituting between 0.44% and 1.87% of all PM chemical compositions (Table S3), thereby revealing the critical roles of the effective variables played on microbial communities despite the small percentages.

CCA and OPLS-DA were conducted on 11 effective variables and 3 indicators (number of all OTUs, Chao index, and Shannon index) of microbial communities to investigate the potential correlation between microbial communities and PM chemical compositions on human facial skin. The results of the CCA and OPLS-DA provided insights into the relationship between the microbial communities and PM chemical compositions (Figures 4 and 5). The first two axes of the CCA had inertia of 1.000, and the correlations between the three indicators and effective variables were 99.3% and 100%, respectively, indicating that the CCA analysis accurately described the relationship between the three indicators and effective variables and that the previous application of Collinearity Diagnostics was successful. The weighted correlation matrix of the CCA showed a strong relationship between the Ace index and OTUs, which was consistent with the definition of the Ace index. Therefore, in the following analysis, only the impacts of PM on the Ace index and Shannon index were analyzed.

As shown in Figures 4 and 5, it can be observed that Chlorobenzene had a minimal impact and contribution on microbial communities across different concentrations of PM and times. On the other hand, p-Xylene showed a positive correlation with the Chao index of microbial communities in higher concentrations of PM. However, InP and BkF displayed a negative correlation, indicating a substantial impact of these chemical compositions with VIP > 1.14. In addition, InP demonstrated a positive correlation with the Shannon index of microbial communities (VIP > 1.06), while p-Xylene was found to have a negative impact, with a VIP > 1.02. In cases of lower concentrations of PM, we observed a positive correlation between Toluene and the richness of microbial communities. Nevertheless, NO<sub>3</sub><sup>-</sup>, 1,2-Dibromoethane, Acen, and especially 1,3,5-Trimethylbenzene (VIP > 1.93), were found to have a negative impact on microbial communities. Further, a positive correlation between p-Xylene and the diversity of microbial communities (VIP > 1.14) was observed, while Ca, especially Toluene (VIP > 1.78), demonstrated a negative correlation with the Shannon index.

Our results also showed that 1,3,5-Trimethylbenzene had a positive influence on the richness of microbial communities in the morning samples (VIP > 1.19), while Cr exerted a negative distinctive impact. Although Acen and BkF, but not Toluene, were found to have a positive impact on the Shannon index, the VIP analysis showed that the impact was not significant. In the evening samples, CCA indicated a positive correlation between the richness of microbial communities and BkF, Ca, and Cr, with VIP > 1.20 except for Toluene and Acen. Further, InP and BkF had a positive impact (VIP > 1.38), while Ca and Cr had a negative and non-significant impact (VIP < 0.88) on the diversity of microbial communities.



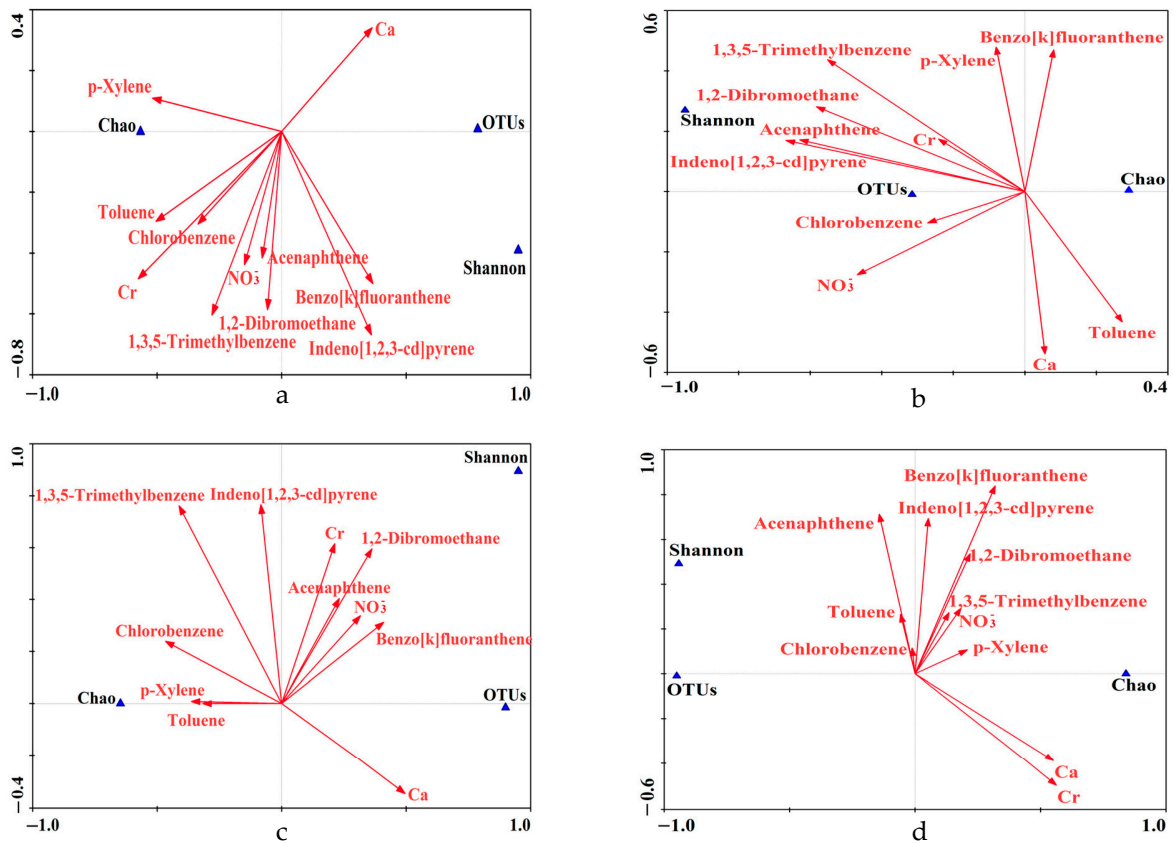


**Figure 4.** The relation between microbial communities diversity and PM chemical compositions in different environmental variables based on CCA. (a) High concentrations of PM; (b) low concentrations of PM; (c) in the morning; (d) in the evening.

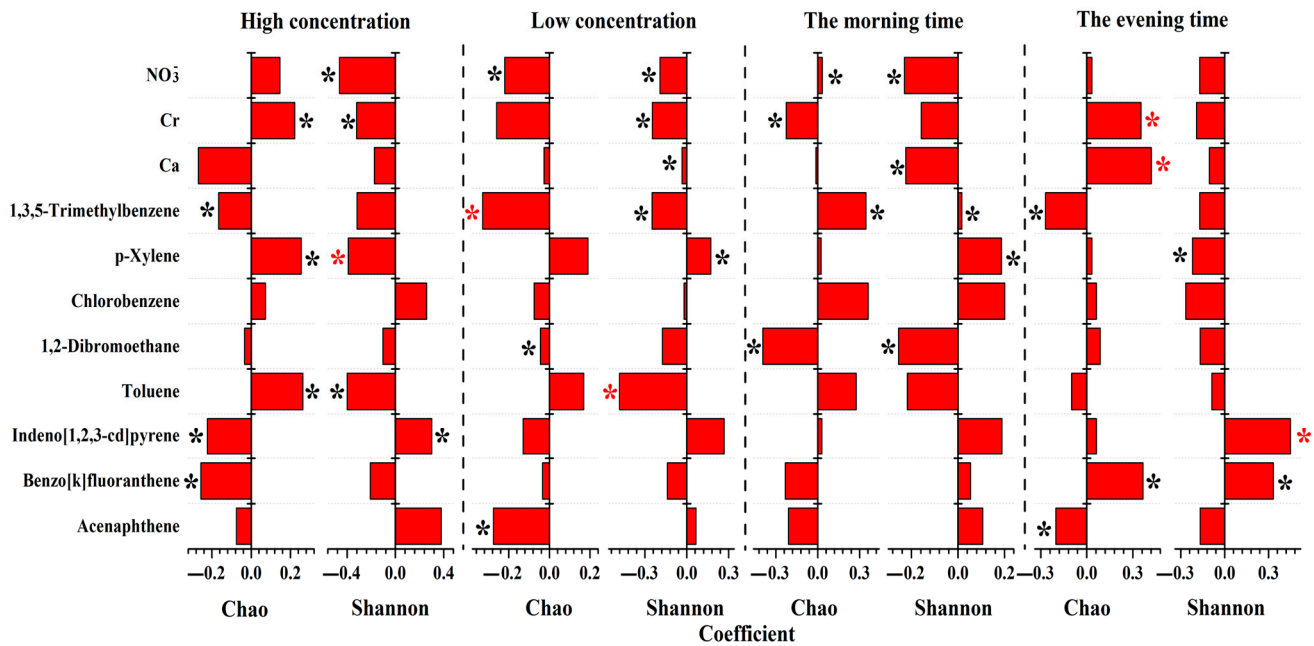


**Figure 5.** The effects of PM chemical compositions on microbial richness/diversity based on OPLS-DA. Chao index indicates microbial richness, and Shannon index indicates microbial diversity. The black and red asterisks indicate the variable importance in the projection (VIP) values exceeding 1 and 1.5, respectively.

### 3.3. Reactive Species Influence Microbial Communities

To further explore the effects of PM chemical compositions on microbial communities, the  $\cdot\text{OH}$  of the most important reactive species was analyzed by EPR. The results showed that the  $\cdot\text{OH}$  concentrations were significantly lower in low PM concentrations compared to those in high PM concentrations ( $p = 0.04$ ). In addition, the  $\cdot\text{OH}$  concentrations increased with time from morning to evening. The correlations between  $\cdot\text{OH}$  and microbial communities, in terms of Chao, Shannon, and OTUs, were calculated using the arbitrary unit of  $\cdot\text{OH}$  in the unit area of the facial skin (Figure 6). The Chao index was found to decrease as the  $\cdot\text{OH}$  concentration increased per unit area of facial skin; the Pearson's correlation coefficients were higher than 0.70 using linearity fitting, indicating that the richness of the microbial community was potentially suppressed to some extent by the  $\cdot\text{OH}$  concentration (Figure 6a). However, the fitting of  $\cdot\text{OH}$  and Shannon index was not significant ( $R^2 < 0.04$ ), indicating that the effects of  $\cdot\text{OH}$  on the diversity of microbial communities were not significant, which conflicted with the Chao index (Figure 6b). A similar phenomenon was observed for  $\cdot\text{OH}$  and OTUs ( $R^2 < 0.40$ ), thereby supporting the results for the effects of  $\cdot\text{OH}$  on microbial communities (Figure 6c).

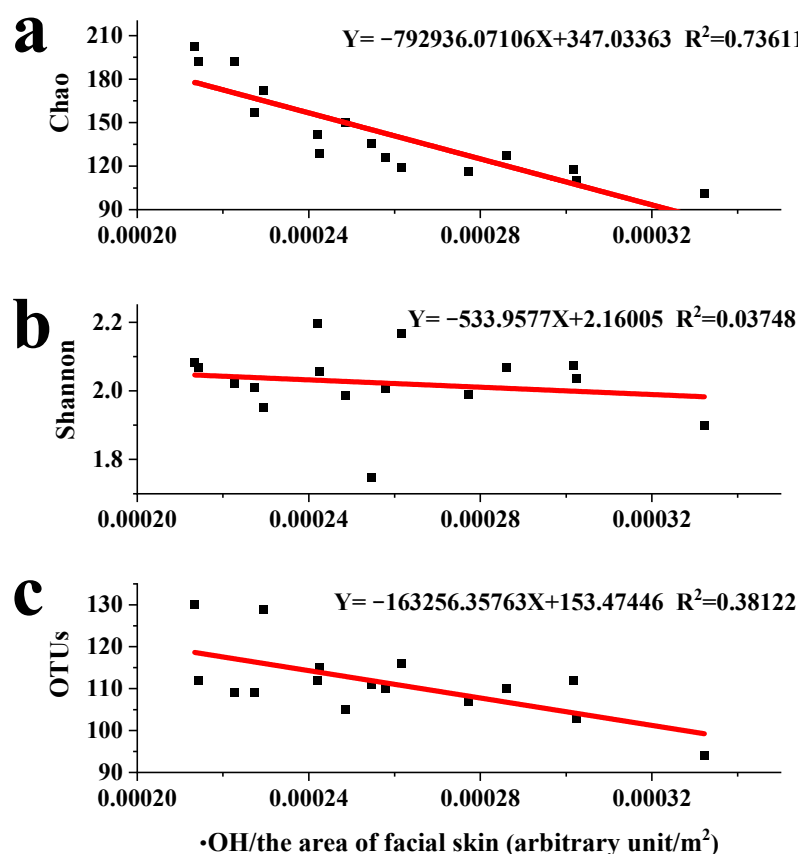


**Figure 6.** The effects of  $\cdot\text{OH}$  on microbial communities. (a–c) The potential effects of  $\cdot\text{OH}$  on richness and diversity indexes Chao, Shannon, and OTUs of microbial communities, respectively.

### 3.4. Health Risks from PM

In this study, human health risk exposure to PM chemical compositions via dermal adsorption was calculated. Cr exhibited the highest non-carcinogenic risk with an HQ exceeding 2.63, which is significantly greater than other PM chemical compositions. Conversely, Toluene had the lowest HQ value ( $1.22 \times 10^{-4}$ ). The HQ of the top three risk contributors (Cr, 1,2-Dibromoethane, and 1,3,5-Trimethylbenzene) decreased in this order for both high and low PM concentrations. Interestingly, this trend was also observed in both morning and evening samples, suggesting that Cr, 1,2-Dibromoethane and 1,3,5-Trimethylbenzene pose a higher non-carcinogenic risk in different environmental variables.

The carcinogenic risk assessment of PM chemical compositions showed that Cr has the highest risk associated with dermal contact, with a mean value of  $29.08 \times 10^{-4}$ , even the minimum value ( $5.98 \times 10^{-4}$ ) exceeds the risk that is unacceptable according to the EPA. The carcinogenic risks of 1,2-Dibromoethane were also confirmed in this study with the mean value of CR was  $5.67 \times 10^{-4}$  (ranging from  $4.74 \times 10^{-5}$  to  $11.61 \times 10^{-4}$ ).

#### 4. Discussion

It is well established that microbial communities are known to shift to some extent in response to changes in environmental variables [47,48]. Moreover, these shifts in microbial communities may often correspond to competitive dynamics that occur when certain bacteria are exposed to ideal (or suboptimal) conditions related to food availability, temperature, humidity, salinity, pH, and other environmental factors [49,50]. This study successfully determined the variability in microbial communities driven by PM and their correlation on human facial skin in different environmental variables based on the characterizations of PM chemical compositions, which was supported by a shift in microbial community structure and PM chemical compositions from the laboratory experiments described above.

The study revealed a higher number of species in high concentrations of PM and during the morning, which was consistent with the Chao index (Figure 2). This phenomenon can be explained by three possible factors. First, it could be possible that some microbes can more easily utilize carbon and energy sources present in high concentrations of PM [14,51]. Second, microbial communities may tend to seek refuge from adverse nighttime atmospheric conditions, such as UV exposure and rapid temperature fluctuations, which could occur while people are sleeping [14]. Third, microbes on human facial skin may propagate more quickly during the night, as they may utilize secretions from the skin that accumulate during sleep [52]. Further, we found that microbial communities closely interacted in high concentrations of PM, as evidenced by the shared OTUs shown in Figure 1, suggesting that the chemical compositions of PM, as well as environmental variables such as airflow, temperature, the availability of suitable food sources, and the presence of human secretions played similar roles in shaping the microbial communities [52]. The larger diversity of microbial communities in high concentrations of PM (Figure 2) indicated that higher concentrations of PM might influence the composition of microbial communities, similar to that documented in a previous study [53]. Additionally, the study revealed that microbial communities exhibited higher richness and lower diversity in the morning compared to the evening (Figure 2), suggesting that microbes thrived more actively during nighttime in milder environmental conditions, which may provide protection against harsh atmospheric factors and foster heterotrophic activity, aligning with findings from previous studies [26,54]. However, during the daytime, factors such as increased airflow, crowd flow, and microbial immigration via airborne dust may contribute to an increase in the diversity of microbial communities due to the introduction of other bacteria [55].

In this study, the analysis of human facial skin samples revealed a predominance of Gram-positive microbes, including a subset of microbial genera (*Lactococcus*, *Bacillus*, and *Arthrobacter*) known to be associated with acid production, which may impact human health and induce skin and intestinal diseases [56,57]. Further, the structural cell wall compositions and thickness of Gram-positive microbes allow them to remain viable for longer durations in the air, which may cause more damage to humans [58]. Despite the observed changes in microbial richness and diversity with significant shifts ( $p < 0.05$ ) from human samples in different environmental variables (Figure 2), the overall stability of the microbial community structure remained relatively unchanged. In particular, dominant bacterial genera such as *Lactococcus* and *Bacillus* did not exhibit significant changes in abundance over time. This finding indicates that microbial communities on human facial skin exhibit stress resistance, enabling them to withstand environmental attenuation, PM-induced toxicity, and natural enemies [59]. Overall, the stability of these microbial communities could be influenced by PM and change substantially over time, characterized by alterations in their richness and diversity, as shown by the CCA and OPLS-DA results.

The concentrations of PM chemical compositions, including heavy metals, water-soluble ions, PAHs, and VOCs, were measured in different environmental samples (Table S3). The results showed that in environments with high concentrations of PM and appropriate temperatures, degrading bacteria could be incubated to degrade p-Xylene for ecological balance, thereby contributing to an increase in the enrichment of microbial communities [60]. In low concentrations of PM, with the presence of Toluene and appropriate environmental conditions, certain microbial species may actively metabolize this compound [61]. Moreover, bacteria can use toluene sulfonate, which is produced from Toluene and sulfate, as the sole source of sulfur, carbon, and electron acceptors to enhance the richness of microbial communities [62]. However, Toluene-degrading bacteria such as *Pseudomonas* are dominant in high-Toluene environments and may reduce microbial diversity [63].

This study showed that the richness of microbial communities correlated with Cr, but opposite results were observed in regard to diversity in the evening. In addition, Cr was found to have an important effect on the assembly of microbial communities, whereas microbial communities could be negatively affected by Cr stress over time by inhibiting most metabolic pathways and functional genes [64,65]. In the present study, the richness of microbial communities increased significantly with Ca, while restricted diversity was observed in the evening, reflecting the dual character of the influence of Ca [66,67].  $\text{NO}_3^-$  played a negative effect on the growth and reproduction of some bacteria, especially basophilic bacteria, similar to that reported in a previous study [68]. The impact may be even more severe in acidic aerosols, where heavy metals and organic matter can recombine and further alter bacterial enzymatic activity and metabolism. Despite this, certain bacteria may still be able to acquire nitrogen nutrition from  $\text{NO}_3^-$  to increase the richness of microbial communities [69].

Our study analysis also revealed that InP positively impacted the diversity of microbial communities across varying concentrations of PM. Additionally, it has been shown that, under appropriate conditions, the introduction of certain bacteria to soil can lead to the depletion of InP, which is crucial in determining the effectiveness of a remedial strategy [70]. As the concentrations of PAHs, particularly high-molecular-weight PAHs such as InP, increase, specific degradation bacteria may emerge to effectively reduce the levels of these pollutants, which can ultimately lead to an increase in the diversity of microbial communities [70]. Additionally, laboratory studies have also shown that BkF is highly effective in enhancing enzyme activity, specifically in the degradation of high-molecular-weight PAHs, thereby significantly increasing the richness and diversity of microbial communities in evening samples [71].

Reactive oxygen species (ROS), highly correlated with organic compounds and transition metals, are thought to cause oxidative stress as the main mechanism of PM toxicity in aerosols [72].  $\cdot\text{OH}$ , an important ROS typically present in the open air, is known to be highly reactive and can cause significant environmental health risks through oxidative damage [73]. The concentrations of  $\cdot\text{OH}$  were found to significantly increase with increased PM concentrations ( $p = 0.04$ ), possibly due to the increase in the effectiveness of organic compounds and transition metals with changing environmental conditions. The concentrations of  $\cdot\text{OH}$  from human facial skin tended to increase after exposure to air in one day, but the difference was not significant ( $p > 0.2$ ). Linear fitting of  $\cdot\text{OH}$  and microbial community indexes exhibited preminent fitting in terms of the Chao index, indicating that  $\cdot\text{OH}$  might play an important role in the enrichment of microbial communities (Figure 6a), possibly due to  $\cdot\text{OH}$  as the production from PM-inhibited bacteria growth and the appearance of new bacteria by oxidative stress [74]. However, the role of  $\cdot\text{OH}$  on microbial community diversity was not obvious. Our results showed that heavy metals and organic compounds might have more effect than  $\cdot\text{OH}$  on microbial community diversity, and recombination action played a more important role on the microbial communities.

HQ, representing non-carcinogenic risk, revealed that Cr, 1,2-Dibromoethane, and 1,3,5-Trimethylbenzene were the top three PM chemical compositions with highest non-carcinogenic risks, which indicated that these PM chemical compositions might pose a

non-carcinogenic risk to humans. The US EPA recommends an acceptable level of  $1 \times 10^{-6}$  as the criterion of health risk identification, whereby values exceeding this threshold indicate a substantial risk [8,39]. However, the carcinogenic risks calculated in our study ranged from  $4.74 \times 10^{-5}$  to  $66.32 \times 10^{-4}$  in different environmental variables, significantly exceeding the acceptable level stated by the US EPA, indicating that the carcinogenic risk from PM (especially Cr and 1,2-Dibromoethane) for residents in the exposed population could be of great concern. The findings of this study suggest that the dermal adsorption of PM chemical compositions poses potential non-carcinogenic and carcinogenic risk that should not be ignored. Furthermore, the health risks show a significant increase when considering the ingestion and inhalation of PM through the mouth and nose. Therefore, greater emphasis is recommended on health risks associated with long-term exposure to PM chemical compositions, and the potential harm to human health should not be overlooked, especially in places with significant air pollution. Thus, it is strongly recommended that air pollution be controlled, and measures for health protection be implemented for residents in affected regions.

## 5. Conclusions

In this study, we analyzed microbial communities in different concentrations of PM and at different times on facial skin. Through high-throughput techniques, we observed a stable community structure and regular richness and diversity of microbial communities, which were confirmed to be impacted by the chemical compositions of PM. Through Collinearity Diagnostics, we identified 11 effective variables from all PM chemical compositions, and the results suggest that Chlorobenzene had a minimal impact and contribution on microbial communities. The richness of microbial communities was positively impacted by VOCs in different concentrations of PM, whereas the diversity of microbial communities was positively impacted by PAHs at different times. Moreover, there was an association between heavy metals, such as Ca and Cr, and altered richness and diversity of microbial community in evening samples. Reactive species analysis revealed that  $\cdot\text{OH}$  and richness of microbial communities had a better linear relationship, although this phenomenon was not observed in terms of diversity.

In conclusion, the variability in microbial communities driven by PM and the stability structure possessed by microbial communities were assessed in this study, which showed that *Lactobacillales*, *Bacillales*, *Solibacillus*, and *Pseudomonadales* were the most abundant bacteria. All estimated health risks from PM chemical compositions, calculated under different environmental variables, significantly exceeded the acceptable level set by the US EPA. Crucially, Cr and 1,2-Dibromoethane were identified as posing dual threats, exhibiting both non-carcinogenic and carcinogenic risks.

Overall, this present study provides in-depth insights into the fundamental mechanisms of the variability in microbial communities driven by PM. Importantly, the findings reveal the potential health risks associated with PM chemical compositions on human facial skin, emphasizing the urgent need for controlling major pollutants and for individuals to take protective measures such as wearing masks or maintaining facial skin cleansing when exposed to open polluted air. These findings offer valuable information for the development of strategies aimed at mitigating the adverse effects of PM on human health.

**Supplementary Materials:** Analytical methods for PM properties and microbial communities; Tables of 16 PAHs and 35 VOCs; Concentrations of the main chemical compositions. The following Supplementary Materials can be downloaded at: <https://www.mdpi.com/article/10.3390/toxics12070497/s1>, Table S1: Summary of 16 PAHs priority pollutant information; Table S2: Summary of 35 VOCs information; Table S3: Concentrations of the main chemical compositions in human facial skin ( $\text{mg}/\text{m}^2$ ). References [75–79] are cited in the Supplementary Materials.

**Author Contributions:** K.F.: Methodology, Investigation, Writing—Original Draft Preparation. Q.Z.: Resources, Conceptualisation, Project administration, Funding acquisition, Formal Analysis,

Writing—Review and Editing. H.W.: Writing—Review and Editing. All authors have read and agreed to the published version of the manuscript.

**Funding:** This work was financially supported by the Ministry of Science and Technology of the People’s Republic of China as a key technology research and development program project (grant No. 2023YFC3709001), the National Natural Science Foundation of China (NSFC) as a Shandong-NSFC joint project (grant No. U1906222), and the Tianjin Science and Technology Bureau as a key science and technology supporting project (grant No. S19ZC60133).

**Institutional Review Board Statement:** The study did not require ethical approval since without pathogenicity for human subjects.

**Informed Consent Statement:** Informed consent was obtained from all subjects involved in the study.

**Data Availability Statement:** The raw data supporting the conclusions of this article will be made available by the authors on request.

**Acknowledgments:** The authors acknowledge the dedication and cooperation of all the participants and Home for Researchers ([www.home-for-researchers.com](http://www.home-for-researchers.com), accessed on 15 May 2024) in this study.

**Conflicts of Interest:** The authors declare no conflict of interest.

## Abbreviations

PM	particulate matter
US EPA	US Environmental Protection Agency
PAHs	polycyclic aromatic hydrocarbons
VOCs	volatile organic compounds
CCA	canonical correspondence analysis
OPLS-DA	orthogonal partial least squares discriminant analysis
·OH	hydroxyl radicals
EPR	electron paramagnetic resonance
CNEMC	China National Environmental Monitoring Centre
PCR	polymerase chain reaction
Operational taxonomic units	OTUs
RDP	Ribosomal Database Project
DMPO	5,5-dimethyl-1-pyrroline-N-oxide
HQ	hazard quotient
CR	carcinogenic risk
SF	slope factor
AF	dermal adherence factors
ABS	dermal absorption factor
SA	skin area
ED	exposure duration
EF	exposure frequency
BW	body weight
AT	averaging time
NaP	naphthalene
Acy	acenaphthylene
Acen	acenaphthene
Fl	fluorene
Phe	phenanthrene
Ant	anthracene
Flu	fluoranthene
Pyr	pyrene
BaA	benzo[a]anthracene
Chr	chrysene
BbF	benzo[b]fluoranthene
BkF	benzo[k]fluoranthene
BaP	benzo[a]pyrene

InP	indeno[1,2,3-cd]pyrene
DbA	dibenzo[a,h]anthracene
BgP	benzo[g,h,i]perylene
VIP	variable importance

## References

- Luo, H.; Guan, Q.; Lin, J.; Wang, Q.; Yang, L.; Tan, Z.; Wang, N. Air pollution characteristics and human health risks in key cities of northwest China. *J. Environ. Manag.* **2020**, *269*, 110791. [[CrossRef](#)] [[PubMed](#)]
- Aguilera, R.; Corringham, T.; Gershunov, A.; Benmarhnia, T. Wildfire smoke impacts respiratory health more than fine particles from other sources: Observational evidence from Southern California. *Nat. Commun.* **2021**, *12*, 1493. [[CrossRef](#)] [[PubMed](#)]
- Jbaily, A.; Zhou, X.D.; Liu, J.; Lee, T.H.; Kamareddine, L.; Verguet, S.; Dominici, F. Air pollution exposure disparities across US population and income groups. *Nature* **2022**, *601*, 228–233. [[CrossRef](#)] [[PubMed](#)]
- Burnett, R.; Chen, H.; Szyszkowicz, M.; Fann, N.; Hubbell, B.; Pope, C.A.; Apte, J.S.; Brauer, M.; Cohen, A.; Weichenthal, S.; et al. Global estimates of mortality associated with long-term exposure to outdoor fine particulate matter. *Proc. Natl. Acad. Sci. USA* **2018**, *115*, 9592–9597. [[CrossRef](#)] [[PubMed](#)]
- Grigorieva, E.; Lukyanets, A. Combined Effect of Hot Weather and Outdoor Air Pollution on Respiratory Health: Literature Review. *Atmosphere* **2021**, *12*, 790. [[CrossRef](#)]
- Li, T.T.; Zhang, Y.; Wang, J.N.; Xu, D.D.; Yin, Z.X.; Chen, H.S.; Lv, Y.B.; Luo, J.S.; Zeng, Y.; Liu, Y.; et al. All-cause mortality risk associated with long-term exposure to ambient PM<sub>2.5</sub> in China: A cohort study. *Lancet Public Health* **2018**, *3*, E470–E477. [[CrossRef](#)]
- Zhang, J.F.; Wei, Y.J.; Fang, Z.F. Ozone Pollution: A Major Health Hazard Worldwide. *Front. Immunol.* **2019**, *10*, 2518. [[CrossRef](#)] [[PubMed](#)]
- Rahman, M.S.; Khan, M.D.H.; Jolly, Y.N.; Kabir, J.; Akter, S.; Salam, A. Assessing risk to human health for heavy metal contamination through street dust in the Southeast Asian Megacity: Dhaka, Bangladesh. *Sci. Total Environ.* **2019**, *660*, 1610–1622. [[CrossRef](#)] [[PubMed](#)]
- Thomas, S.; Izard, J.; Walsh, E.; Batich, K.; Chongsathidkiet, P.; Clarke, G.; Sela, D.A.; Muller, A.J.; Mullin, J.M.; Albert, K.; et al. The Host Microbiome Regulates and Maintains Human Health: A Primer and Perspective for Non-Microbiologists. *Cancer Res.* **2017**, *77*, 1783–1812. [[CrossRef](#)]
- Manus, M.B.; Yu, J.J.; Park, L.P.; Mueller, O.; Windsor, S.C.; Horvath, J.E.; Nunn, C.L. Environmental influences on the skin microbiome of humans and cattle in rural Madagascar. *Evol. Med. Public Health* **2017**, *2017*, 144–153. [[CrossRef](#)]
- Chen, C.Y.; He, R.Q.; Cheng, Z.Y.; Han, M.Z.; Zha, Y.G.; Yang, P.S.; Yao, Q.; Zhou, H.; Zhong, C.F.; Ning, K. The Seasonal Dynamics and the Influence of Human Activities on Campus Outdoor Microbial Communities. *Front. Microbiol.* **2019**, *10*, 1579. [[CrossRef](#)] [[PubMed](#)]
- Flies, E.J.; Clarke, L.J.; Brook, B.W.; Jones, P. Urbanisation reduces the abundance and diversity of airborne microbes—But what does that mean for our health? A systematic review. *Sci. Total Environ.* **2020**, *738*, 140337. [[CrossRef](#)]
- Lloyd-Price, J.; Arze, C.; Ananthakrishnan, A.N.; Schirmer, M.; Avila-Pacheco, J.; Poon, T.W.; Andrews, E.; Ajami, N.J.; Bonham, K.S.; Brislawn, C.J.; et al. Multi-omics of the gut microbial ecosystem in inflammatory bowel diseases. *Nature* **2019**, *569*, 655–662. [[CrossRef](#)] [[PubMed](#)]
- Zhou, Q.; Fu, K.; Hu, X.; Li, X.; Lai, Z.; Yuan, P. Relationships between Airborne Microbial Community Diversity, Heating Supply Patterns and Particulate Matter Properties. *J. Environ. Chem. Eng.* **2022**, *10*, 107309. [[CrossRef](#)]
- Sun, Y.J.; Xu, S.W.; Zheng, D.Y.; Li, J.; Tian, H.Z.; Wang, Y. Effects of haze pollution on microbial community changes and correlation with chemical components in atmospheric particulate matter. *Sci. Total Environ.* **2018**, *637*, 507–516. [[CrossRef](#)] [[PubMed](#)]
- Du, P.R.; Du, R.; Ren, W.S.; Lu, Z.D.; Fu, P.Q. Seasonal variation characteristic of inhalable microbial communities in PM<sub>2.5</sub> in Beijing city, China. *Sci. Total Environ.* **2018**, *610*, 308–315. [[CrossRef](#)] [[PubMed](#)]
- Chen, X.; Zhao, Y.; Zhao, X.; Wu, J.; Zhu, L.; Zhang, X.; Wei, Z.; Liu, Y.; He, P. Selective pressures of heavy metals on microbial community determine microbial functional roles during composting: Sensitive, resistant and actor. *J. Hazard. Mater.* **2020**, *398*, 122858. [[CrossRef](#)]
- Wu, M.; Guo, X.; Wu, J.; Chen, K. Effect of compost amendment and bioaugmentation on PAH degradation and microbial community shifting in petroleum-contaminated soil. *Chemosphere* **2020**, *256*, 126998. [[CrossRef](#)]
- McBride, S.G.; Osburn, E.D.; Lucas, J.M.; Simpson, J.S.; Brown, T.; Barrett, J.E.; Strickland, M.S. Volatile and Dissolved Organic Carbon Sources Have Distinct Effects on Microbial Activity, Nitrogen Content, and Bacterial Communities in Soil. *Microb. Ecol.* **2022**, *85*, 659–668. [[CrossRef](#)]
- Zhang, X.H.; Li, Z.Y.; Hu, J.M.; Yan, L.; He, Y.Y.; Li, X.; Wang, M.Y.; Sun, X.M.; Xu, H. The biological and chemical contents of atmospheric particulate matter and implication of its role in the transmission of bacterial pathogenesis. *Environ. Microbiol.* **2021**, *23*, 5481–5486. [[CrossRef](#)]
- Liu, Y.C.; Zuo, Z.Q.; Li, H.; Xing, Y.X.; Cheng, D.; Guo, M.; Liu, T.; Zheng, M.; Yuan, Z.G.; Huang, X. In-situ advanced oxidation of sediment iron for sulfide control in sewers. *Water Res.* **2023**, *240*, 120077. [[CrossRef](#)] [[PubMed](#)]

22. Ma, W.; Han, R.; Zhang, W.; Zhang, H.; Zhao, L.; Chen, L.; Zhu, L. Advanced oxidation process/coagulation coupled with membrane distillation (AOP/Coag-MD) for efficient ammonia recovery: Elucidating biofouling control performance and mechanism. *J. Hazard. Mater.* **2024**, *469*, 134093. [[CrossRef](#)]
23. Chen, H.; Du, R.; Zhang, Y.; Zhang, S.; Ren, W.; Du, P. Survey of background microbial index in inhalable particles in Beijing. *Sci. Total Environ.* **2021**, *757*, 143743. [[CrossRef](#)]
24. Sun, Y.J.; Huang, Y.J.; Xu, S.W.; Li, J.; Yin, M.; Tian, H.Z. Seasonal Variations in the Characteristics of Microbial Community Structure and Diversity in Atmospheric Particulate Matter from Clean Days and Smoggy Days in Beijing. *Microb. Ecol.* **2022**, *83*, 568–582. [[CrossRef](#)]
25. Qin, N.; Liang, P.; Wu, C.Y.; Wang, G.Q.; Xu, Q.; Xiong, X.; Wang, T.T.; Zolfo, M.; Segata, N.; Qin, H.L.; et al. Longitudinal survey of microbiome associated with particulate matter in a megacity. *Genome Biol.* **2020**, *21*, 55. [[CrossRef](#)]
26. Hu, Z.; Liu, H.; Zhang, H.; Zhang, X.; Zhou, M.; Lou, L.; Zheng, P.; Xi, C.; Hu, B. Temporal discrepancy of airborne total bacteria and pathogenic bacteria between day and night. *Environ. Res.* **2020**, *186*, 109540. [[CrossRef](#)] [[PubMed](#)]
27. Daellenbach, K.R.; Uzu, G.; Jiang, J.H.; Cassagnes, L.E.; Leni, Z.; Vlachou, A.; Stefanelli, G.; Canonaco, F.; Weber, S.; Segers, A.; et al. Sources of particulate-matter air pollution and its oxidative potential in Europe. *Nature* **2020**, *587*, 414–419. [[CrossRef](#)] [[PubMed](#)]
28. Gunthe, S.S.; Liu, P.F.; Panda, U.; Raj, S.S.; Sharma, A.; Darbyshire, E.; Reyes-Villegas, E.; Allan, J.; Chen, Y.; Wang, X.; et al. Enhanced aerosol particle growth sustained by high continental chlorine emission in India. *Nat. Geosci.* **2021**, *14*, 77–84. [[CrossRef](#)]
29. Zhu, Q.; Liu, Y.; Hasheminassab, S. Long-term source apportionment of PM<sub>2.5</sub> across the contiguous United States (2000–2019) using a multilinear engine model. *J. Hazard. Mater.* **2024**, *472*, 134550. [[CrossRef](#)]
30. Fan, S.M.; Xia, B.; Liu, W.X.; Yu, W.; Wu, Z.X.; Chen, S.B.; Liu, Q.H.; Chen, W.J.; Zhu, S.L.; Jin, M.; et al. Establishing an appropriate Z score regression equation for Chinese pediatric coronary artery echocardiography: A multicenter prospective cohort study. *BMC Pediatr.* **2021**, *21*, 429. [[CrossRef](#)]
31. Wu, Q.; Zhou, Y.; Fan, X.; Ma, H.; Gu, W.R.; Sun, F.J. Evaluation of nine formulas for estimating the body surface area of children with hematological malignancies. *Front. Pediatr.* **2022**, *10*, 989049. [[CrossRef](#)] [[PubMed](#)]
32. Henriksson, A.; Kuo, K.; Gerken, K.; Cline, K.; Hespel, A.-M.; Cole, R.; Moon, R. Body mapping chart for estimation of percentage of body surface area in mesocephalic dogs. *J. Vet. Emerg. Crit. Care* **2022**, *32*, 350–355. [[CrossRef](#)] [[PubMed](#)]
33. Choi, J.; Patil, A.; Vendrow, E.; Touponse, G.; Aboukhater, L.; Forrester, J.D.; Spain, D.A. Practical Computer Vision Application to Compute Total Body Surface Area Burn Reappraising a Fundamental Burn Injury Formula in the Modern Era. *JAMA Surg.* **2022**, *157*, 129–135. [[CrossRef](#)] [[PubMed](#)]
34. Sharma, P.; Tripathi, S.; Chandra, R. Metagenomic analysis for profiling of microbial communities and tolerance in metal-polluted pulp and paper industry wastewater. *Bioresour. Technol.* **2021**, *324*, 124681. [[CrossRef](#)] [[PubMed](#)]
35. Bukin, Y.S.; Galachyants, Y.P.; Morozov, I.V.; Bukin, S.V.; Zakharenko, A.S.; Zemskaya, T.I. The effect of 16S rRNA region choice on bacterial community metabarcoding results. *Sci. Data* **2019**, *6*, 190007. [[CrossRef](#)]
36. Li, Z.; Yang, W.; Xie, L.; Li, Y.; Liu, Y.; Sun, Y.; Bu, Y.; Mi, X.; Zhan, S.; Hu, W. Prominent role of oxygen vacancy for superoxide radical and hydroxyl radical formation to promote electro-Fenton like reaction by W-doped CeO<sub>2</sub> composites. *Appl. Surf. Sci.* **2021**, *549*, 149262. [[CrossRef](#)]
37. Wang, D.; Wu, H.; Wang, C.; Gu, L.; Chen, H.; Jana, D.; Feng, L.; Liu, J.; Wang, X.; Xu, P.; et al. Self-Assembled Single-Site Nanozyme for Tumor-Specific Amplified Cascade Enzymatic Therapy. *Angew. Chem. Int. Ed. Engl.* **2021**, *60*, 3001–3007. [[CrossRef](#)]
38. Zhou, Q.; Song, C.; Wang, P.; Zhao, Z.; Li, Y.; Zhan, S. Generating dual-active species by triple-atom sites through peroxy-monosulfate activation for treating micropollutants in complex water. *Proc. Natl. Acad. Sci. USA* **2023**, *120*, e2300085120. [[CrossRef](#)]
39. Tao, H.; Wang, Y.J.; Liang, H.H.; Zhang, X.H.; Liu, X.P.; Li, J.L. Pollution characteristics of phthalate acid esters in agricultural soil of Yinchuan, northwest China, and health risk assessment. *Environ. Geochem. Health* **2020**, *42*, 4313–4326. [[CrossRef](#)]
40. Santamouris, M.; Synnefa, A.; Assimakopoulos, M.; Livada, I.; Pavlou, K.; Papaglastra, M.; Gaitani, N.; Kolokotsa, D.; Assimakopoulos, V. Experimental investigation of the air flow and indoor carbon dioxide concentration in classrooms with intermittent natural ventilation. *Energy Build.* **2008**, *40*, 1833–1843. [[CrossRef](#)]
41. U.S. Environmental Protection Agency (USEPA). Integrated Risk Information System (Electronic Data Base). 2002. Available online: <http://www.epa.gov/iris> (accessed on 25 June 2024).
42. Pragg, C.; Mohammed, F.K. Distribution and health risk assessment of heavy metals in road dust from an industrial estate in Trinidad, West Indies. *Int. J. Environ. Health Res.* **2020**, *30*, 336–343. [[CrossRef](#)]
43. Wang, R.; Liu, G.; Zhang, J. Variations of emission characterization of PAHs emitted from different utility boilers of coal-fired power plants and risk assessment related to atmospheric PAHs. *Sci. Total Environ.* **2015**, *538*, 180–190. [[PubMed](#)]
44. Li, X.; Shang, X.; Luo, T.; Du, X.; Wang, Y.; Xie, Q.; Matsuura, N.; Chen, J.; Kadokami, K. Screening and health risk of organic micropollutants in rural groundwater of Liaodong Peninsula, China. *Environ. Pollut.* **2016**, *218*, 739–748. [[CrossRef](#)] [[PubMed](#)]
45. Mndela, M.; Madakadze, C.I.; Nherera-Chokuda, F.; Dube, S. Is the soil seed bank a reliable source for passive restoration of bush-cleared semi-arid rangelands of South Africa? *Ecol. Process.* **2020**, *9*, 1. [[CrossRef](#)]
46. Borrego, S.; Vivar, I.; Molina, A. Air- and dustborne fungi in repositories of the National Archive of the Republic of Cuba. *Microb. Cell* **2022**, *9*, 103–122. [[CrossRef](#)] [[PubMed](#)]



47. Ju, F.; Lau, F.; Zhang, T. Linking Microbial Community, Environmental Variables, and Methanogenesis in Anaerobic Biogas Digesters of Chemically Enhanced Primary Treatment Sludge. *Environ. Sci. Technol.* **2017**, *51*, 3982–3992. [[CrossRef](#)] [[PubMed](#)]
48. Liu, J.; Chen, X.; Shu, H.-y.; Lin, X.-r.; Zhou, Q.-x.; Bramryd, T.; Shu, W.-s.; Huang, L.-n. Microbial community structure and function in sediments from e-waste contaminated rivers at Guiyu area of China. *Environ. Pollut.* **2018**, *235*, 171–179. [[PubMed](#)]
49. Xu, C.; Chen, H.; Liu, Z.; Sui, G.; Li, D.; Kan, H.; Zhao, Z.; Hu, W.; Chen, J. The decay of airborne bacteria and fungi in a constant temperature and humidity test chamber. *Environ. Int.* **2021**, *157*, 106816. [[CrossRef](#)]
50. Hou, Z.; Zhou, Q.; Mo, F.; Kang, W.; Ouyang, S. Enhanced carbon emission driven by the interaction between functional microbial community and hydrocarbons: An enlightenment for carbon cycle. *Sci. Total Environ.* **2023**, *867*, 161402. [[CrossRef](#)]
51. Zhang, Y.; Guo, C.; Ma, K.; Tang, A.; Goulding, K.; Liu, X. Characteristics of airborne bacterial communities across different PM<sub>2.5</sub> levels in Beijing during winter and spring. *Atmos. Res.* **2022**, *273*, 106179. [[CrossRef](#)]
52. Meadow, J.F.; Altrichter, A.E.; Bateman, A.C.; Stenson, J.; Brown, G.Z.; Green, J.L.; Bohannon, B. Humans differ in their personal microbial cloud. *PeerJ* **2015**, *3*, e1258. [[CrossRef](#)] [[PubMed](#)]
53. Qi, Y.; Li, Y.; Xie, W.; Lu, R.; Mu, F.; Bai, W.; Du, S. Temporal-spatial variations of fungal composition in PM<sub>2.5</sub> and source tracking of airborne fungi in mountainous and urban regions. *Sci. Total Environ.* **2020**, *708*, 135027. [[CrossRef](#)]
54. Kelly, L.W.; Nelson, C.E.; Haas, A.F.; Naliboff, D.S.; Calhoun, S.; Carlson, C.A.; Edwards, R.A.; Fox, M.D.; Hatay, M.; Johnson, M.D.; et al. Diel population and functional synchrony of microbial communities on coral reefs. *Nat. Commun.* **2019**, *10*, 1691. [[CrossRef](#)] [[PubMed](#)]
55. Yan, D.; Zhang, T.; Su, J.; Zhao, L.L.; Wang, H.; Fang, X.M.; Zhang, Y.Q.; Liu, H.Y.; Yu, L.Y. Structural Variation in the Bacterial Community Associated with Airborne Particulate Matter in Beijing, China, during Hazy and Nonhazy Days. *Appl. Environ. Microbiol.* **2018**, *84*, e00004-18. [[CrossRef](#)] [[PubMed](#)]
56. Balato, A.; Cacciapuoti, S.; Di Caprio, R.; Marasca, C.; Masarà, A.; Raimondo, A.; Fabbrocini, G. Human Microbiome: Composition and Role in Inflammatory Skin Diseases. *Arch. Immunol. Ther. Exp.* **2019**, *67*, 1–18. [[CrossRef](#)] [[PubMed](#)]
57. Casterline, B.W.; Paller, A.S. Early development of the skin microbiome: Therapeutic opportunities. *Pediatr. Res.* **2021**, *90*, 731–737. [[CrossRef](#)]
58. Pasquina-Lemonche, L.; Burns, J.; Turner, R.D.; Kumar, S.; Tank, R.; Mullin, N.; Wilson, J.S.; Chakrabarti, B.; Bullough, P.A.; Foster, S.J.; et al. The architecture of the Gram-positive bacterial cell wall. *Nature* **2020**, *582*, 294–297. [[CrossRef](#)]
59. Kelsic, E.D.; Zhao, J.; Vetsigian, K.; Kishony, R. Counteraction of antibiotic production and degradation stabilizes microbial communities. *Nature* **2015**, *521*, 516–519. [[CrossRef](#)] [[PubMed](#)]
60. Sperfeld, M.; Rauschenbach, C.; Diekert, G.; Studenik, S. Microbial community of a gasworks aquifer and identification of nitrate-reducing *Azoarcus* and *Georgfuchsia* as key players in BTEX degradation. *Water Res.* **2018**, *132*, 146–157.
61. Gholami, F.; Mosmeri, H.; Shavandi, M.; Dastgheib, S.M.M.; Amoozegar, M.A. Application of encapsulated magnesium peroxide (MgO<sub>2</sub>) nanoparticles in permeable reactive barrier (PRB) for naphthalene and toluene bioremediation from groundwater. *Sci. Total Environ.* **2019**, *655*, 633–640. [[CrossRef](#)]
62. Shu, W.; Zhang, Y.; Wen, D.; Wu, Q.; Liu, H.; Cui, M.-H.; Fu, B.; Zhang, J.; Yao, Y. Anaerobic biodegradation of levofloxacin by enriched microbial consortia: Effect of electron acceptors and carbon source. *J. Hazard. Mater.* **2021**, *414* (Suppl. S4), 125520. [[PubMed](#)]
63. Gao, M.; Li, L.; Liu, J. Simultaneous removal of hydrogen sulfide and toluene in a bioreactor: Performance and characteristics of microbial community. *J. Environ. Sci.* **2011**, *23*, 353–359.
64. Sun, F.-L.; Fan, L.-L.; Wang, Y.-S.; Huang, L.-Y. Metagenomic analysis of the inhibitory effect of chromium on microbial communities and removal efficiency in A<sub>2</sub>O sludge. *J. Hazard. Mater.* **2019**, *368*, 523–529. [[PubMed](#)]
65. Araujo, A.S.F.; Miranda, A.R.L.; Pereira, A.P.d.A.; de Melo, W.J.; Melo, V.M.M.; Ventura, S.H.; Brito Junior, E.S.; de Medeiros, E.V.; Araujo, F.F.; Mendes, L.W. Microbial communities in the rhizosphere of maize and cowpea respond differently to chromium contamination. *Chemosphere* **2023**, *313*, 137417. [[PubMed](#)]
66. Hahm, M.S.; Son, J.S.; Kim, B.S.; Ghim, S.Y. Comparative study of rhizobacterial communities in pepper greenhouses and examination of the effects of salt accumulation under different cropping systems. *Arch. Microbiol.* **2017**, *199*, 303–315. [[CrossRef](#)] [[PubMed](#)]
67. Muhammad, N.; Brookes, P.C.; Wu, J. Addition impact of biochar from different feed stocks on microbial community and available concentrations of elements in a Psammaquent and a Plinthudult. *J. Soil Sci. Plant Nutr.* **2016**, *16*, 137–153.
68. Albina, P.; Durban, N.; Bertron, A.; Albrecht, A.; Robinet, J.C.; Erable, B. Influence of Hydrogen Electron Donor, Alkaline pH, and High Nitrate Concentrations on Microbial Denitrification: A Review. *Int. J. Mol. Sci.* **2019**, *20*, 5163. [[CrossRef](#)] [[PubMed](#)]
69. Sun, Y.; Wang, M.; Mur, L.; Shen, Q.; Guo, S. Unravelling the Roles of Nitrogen Nutrition in Plant Disease Defences. *Int. J. Mol. Sci.* **2020**, *21*, 572. [[CrossRef](#)]
70. Huang, R.Y.; Tian, W.J.; Liu, Q.; Yu, H.B.; Jin, X.; Zhao, Y.G.; Zhou, Y.H.; Feng, G. Enhanced biodegradation of pyrene and indeno(1,2,3-cd)pyrene using bacteria immobilized in cinder beads in estuarine wetlands. *Mar. Pollut. Bull.* **2016**, *102*, 128–133. [[CrossRef](#)]
71. Liu, R.; Zhao, L.; Jin, C.; Xiao, N.; Jadeja, R.N.; Sun, T. Enzyme Responses to Phytoremediation of PAH-Contaminated Soil Using *Echinacea purpurea* (L.). *Water Air Soil Pollut.* **2014**, *225*, 2230.
72. Fang, T.; Lakey, P.; Weber, R.J.; Shiraiwa, M. Oxidative Potential of Particulate Matter and Generation of Reactive Oxygen Species in Epithelial Lining Fluid. *Environ. Sci. Technol.* **2019**, *53*, 12784–12792. [[CrossRef](#)]

73. Li, X.; Kuang, X.M.; Yan, C.; Ma, S.; Paulson, S.E.; Zhu, T.; Zhang, Y.; Zheng, M. Oxidative Potential by PM<sub>2.5</sub> in the North China Plain: Generation of Hydroxyl Radical. *Environ. Sci. Technol.* **2019**, *53*, 512–520. [[CrossRef](#)] [[PubMed](#)]
74. Du, P.; Rui, D.; Lu, Z.; Ren, W.; Fu, P. Variation of Bacterial and Fungal Community Structures in PM<sub>2.5</sub> Collected during the 2014 APEC Summit Periods. *Aerosol Air Qual. Res.* **2018**, *18*, 444–455. [[CrossRef](#)]
75. Atzei, D.; Fermo, P.; Vecchi, R.; Fantauzzi, M.; Comite, V.; Valli, G.; Cocco, F.; Rossi, A. Composition and origin of PM<sub>2.5</sub> in Mediterranean Countryside. *Environ. Pollut.* **2019**, *246*, 294–302. [[CrossRef](#)] [[PubMed](#)]
76. Bai, L.; He, Z.; Ni, S.; Chen, W.; Li, N.; Sun, S. Investigation of PM<sub>2.5</sub> absorbed with heavy metal elements, source apportionment and their health impacts in residential houses in the North-east region of China. *Sustain. Cities Soc.* **2019**, *51*, 101690. [[CrossRef](#)]
77. Lin, Y.-C.; Li, Y.-C.; Amesho, K.T.T.; Chou, F.-C.; Cheng, P.-C. Characterization and quantification of PM<sub>2.5</sub> emissions and PAHs concentration in PM<sub>2.5</sub> from the exhausts of diesel vehicles with various accumulated mileages. *Sci. Total Environ.* **2019**, *660*, 188–198.
78. Niu, Y.; Wang, F.; Liu, S.; Zhang, W. Source analysis of heavy metal elements of PM<sub>2.5</sub> in canteen in a university in winter. *Atmos. Environ.* **2021**, *244*, 117879. [[CrossRef](#)]
79. Idris, S.A.'A.; Hanafiah, M.M.; Khan, M.F.; Hamid, H.H.A. Indoor generated PM<sub>2.5</sub> compositions and volatile organic compounds: Potential sources and health risk implications. *Chemosphere* **2020**, *255*, 126932. [[CrossRef](#)]

**Disclaimer/Publisher's Note:** The statements, opinions and data contained in all publications are solely those of the individual author(s) and contributor(s) and not of MDPI and/or the editor(s). MDPI and/or the editor(s) disclaim responsibility for any injury to people or property resulting from any ideas, methods, instructions or products referred to in the content.